Supporting Information

Phase selectivity triggered by nanoconfinement: the impact of corral dimensions

Yi Hu,[a,b] Ana M. Bragança,[a] Lander Verstraete,[a] Oleksandr Ivasenko,[a] Brandon E. Hirsch,[a] Kazukuni Tahara,[c,d] Yoshito Tobe,[c] and Steven De Feyter*[a]

[a] *Department of Chemistry, Division of Molecular Imaging and Photonics, KU Leuven, Celestijnenlaan 200F, B-3001 Leuven, Belgium.*

[b] *College of Materials Science and Engineering, South China University of Technology, Guangzhou 510640, China.*

[c] *Department of Applied Chemistry, School of Science and Technology, Meiji University, 1-1-1 Higashimita, Tama-ku, Kawasaki, 214-8571, Japan.*

[d] *Division of Frontier Materials Science, Graduate School of Engineering Science, Osaka University, Toyonaka, Osaka 560-8531, Japan.*

Corresponding author:

steven.defeyter@kuleuven.be

S1. Experimental section S2

S2. Porous and non-porous structures for DBA-OC13 ..... S3

S3. Data analysis details S4

S4. Concentration dependence phase behaviour for DBA-OC13 on pristine HOPG S6

S5. Experimental details on corral fabrication S9

S.6 Surface coverage of DBA-OC13 in corrals of different sizes S11

S.7 Concentration dependence phase behaviour for DBA-OC12 on pristine HOPG S15

S.8 Surface coverage of DBA-OC12 in corrals of different sizes S16

S.9 Self-assembly of DBA-OC13 in circular and triangular corrals S18

S.10 Stability of nanoconfined DBA-OC13 over time S19

S.11 Data for *in situ* nanoshaving at elevated temperature S20

S.12 Control experiment – Dependence on the nanoshaving direction S21

S.13 References S23

S1. Experimental section

S1.1 Synthesis of DBA

The DBA derivatives used in this study were synthesized according to a previously reported method.[1, 2]

S1.2 STM investigation

All STM experiments were conducted at ambient conditions (temperature: 20–23 ºC; humidity: 40%–50%) using a PicoLE system operating in constant current mode. STM tips were mechanically cut from Pt/Ir (80% / 20%, diameter: 0.25 nm) wire. Stock solutions of achiral DBA derivatives were prepared in 1-phenyloctane (98%, Sigma Aldrich; 6.7×10^{-4} M), and further diluted to the desired concentration. Small amounts of DBA solutions (at varied concentrations) were deposited on a freshly cleaved or covalently modified highly oriented pyrolytic graphite (CM-HOPG) (grade ZYB, Advanced Ceramics Inc., Cleveland, OH, USA) substrate. The experiments were repeated in 2-3 sessions using different tips to check for reproducibility. STM data analysis was executed using either WSxM 5.0 or Scanning Probe Imaging Processor software (SPIP, Image Metrology ApS). Scanning parameters are indicated in figure captions and expressed as V_s for the sample bias and I_t for the tunneling current. The structural models for porous and non-porous structures corresponding to the high-resolution STM images were built using Materials Studio 7.0.

S2. Porous and non-porous structures for DBA-OC13

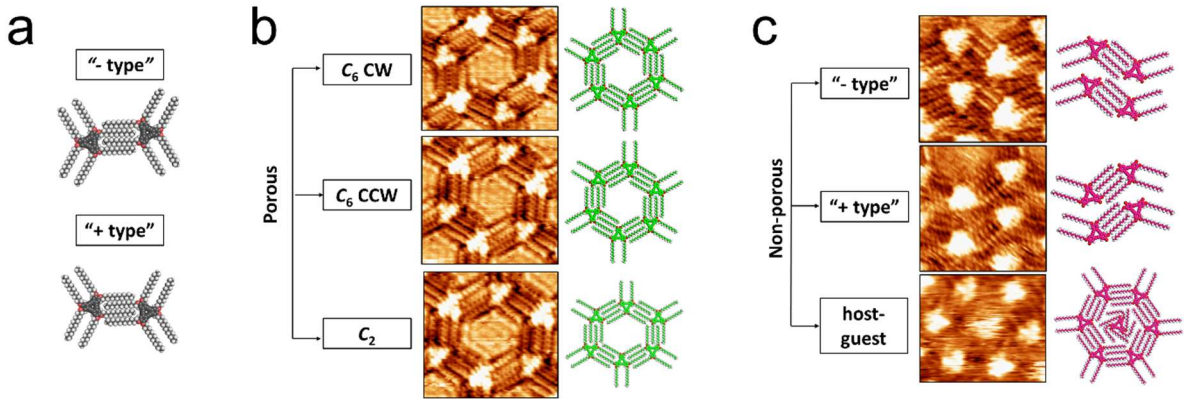

Figure S1. STM images and structural models of the most abundant porous and non-porous structures observed. (a) Dimer interdigitation patterns can be classified as "– type" or "+ type" depending on the relative position of the alkyl chains. (b) Exclusive "– type" or "+ type" dimer interdigitation gives rise to clockwise (CW) and counterclockwise (CCW) pores with C_6-symmetry, respectively. To a lesser extent, linear combinations of both dimer interdigitation patterns generate distorted hexagonal pores with lower symmetry (C_2). (c) The non-porous phase is composed by linear domains exhibiting exclusively "– type" or "+ type" alkyl interdigitation patterns, and the occasional formation of auto host-guest complexes that display a similar molecular density to the linear pattern. Areas that appear fuzzy and/or ill-defined are classified as "defect" areas.

S3. Data analysis details

Determination of the surface coverage of the porous and non-porous structures, and defects in the monolayer was performed while using SPIP^{TM} software. The specific procedure followed depends on the layer morphology.

If the supramolecular pores are isolated, the surface coverage of the porous structure is calculated by first identifying all individual supramolecular pores (green dots in Figure S2). Then for each of these pores, the "pore" area is measured in the following way: in the SPIP software, the area of the hexagon formed by connecting the centers of the six DBA cores is measured. This procedure allows to determine the relative surface coverage of the porous structure, and avoids any systematic errors resulting from imaging artefacts. This procedure was followed for the analysis of the STM images of the self-assembly of DBA-OC13 at the 1-phenyloctane/graphite interface, for concentrations ranging between 6.7×10^{-4} M and 5.6×10^{-6} M (see Figure S2).

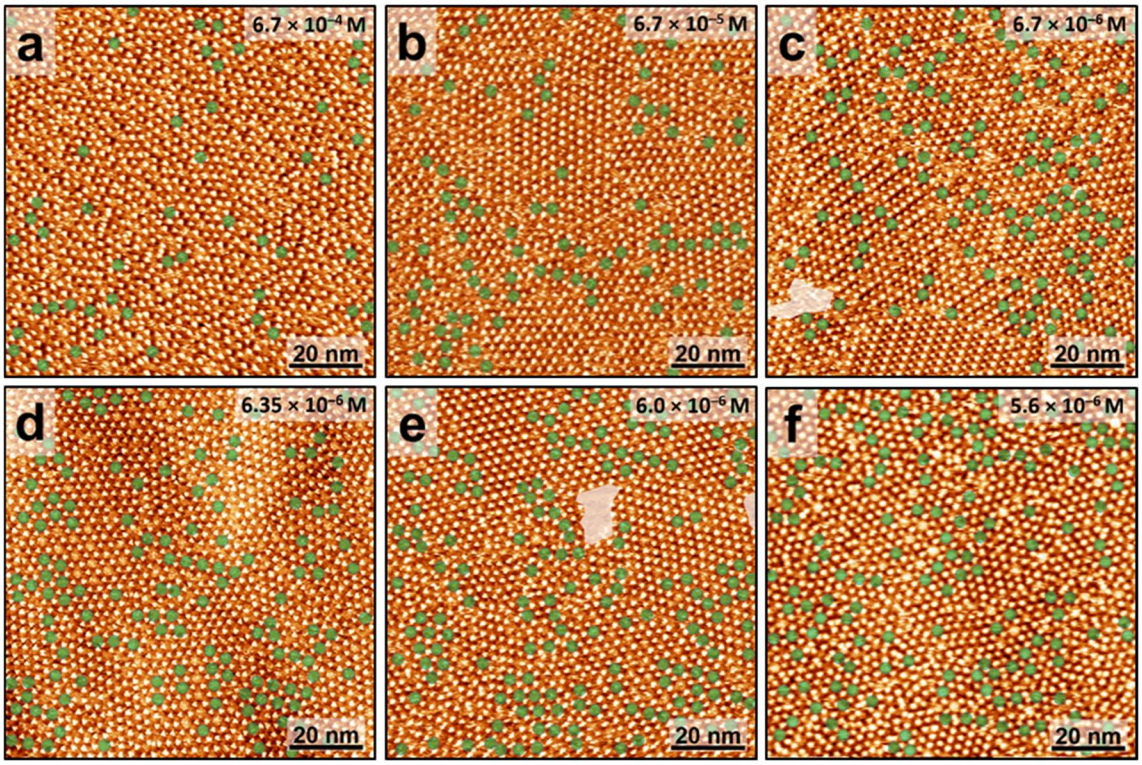

Figure S2. Large-scale STM images for the self-assembly of DBA-OC13 at different concentrations at the 1-phenyloctane/graphite interface. The non-porous structure is dominant on the surface. The hexagonal pores localized among the non-porous structure are indicated by green dots. Scanning parameters: V_s = –0.20 V, I_t = 300 pA.

At lower concentrations (6.7×10^{-7} M – 5.36×10^{-6} M), the porous phase forms more extended domains. In this case both the porous and the non-porous phase can be easily tracked using the SPIP™ software area selection tools. The same protocol holds for the ill-defined areas classified as "defect" areas (white overlay) (see Figure S3).

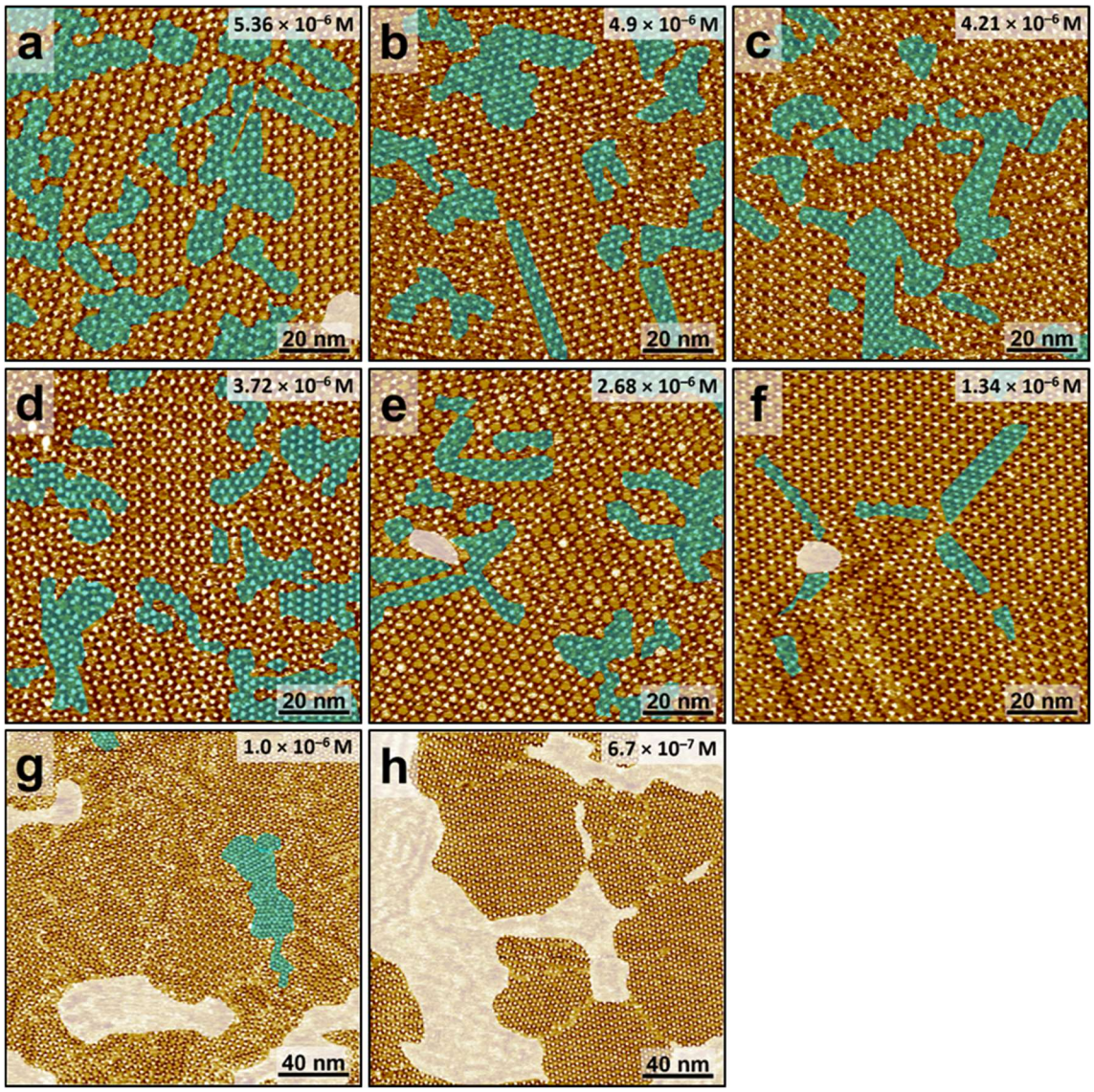

Figure S3 Large-scale STM images of the self-assembly of DBA-OC13 at different concentrations at the 1-phenyloctane/graphite interface. The porous structure is dominant on the surface. The non-porous phase is delimited by the fainted blue areas while defects in the monolayer are covered in white. Scanning parameters: V_s = –0.20 V, I_t = 300 pA.

S4. Concentration dependence phase behaviour for DBA-OC13 on pristine HOPG

For every concentration studied, typically 7 to 30 images obtained during 2-3 experimental sessions were used for the porous/non-porous surface coverage determination. Each point represents an average value, while the error bars represent the standard deviation.

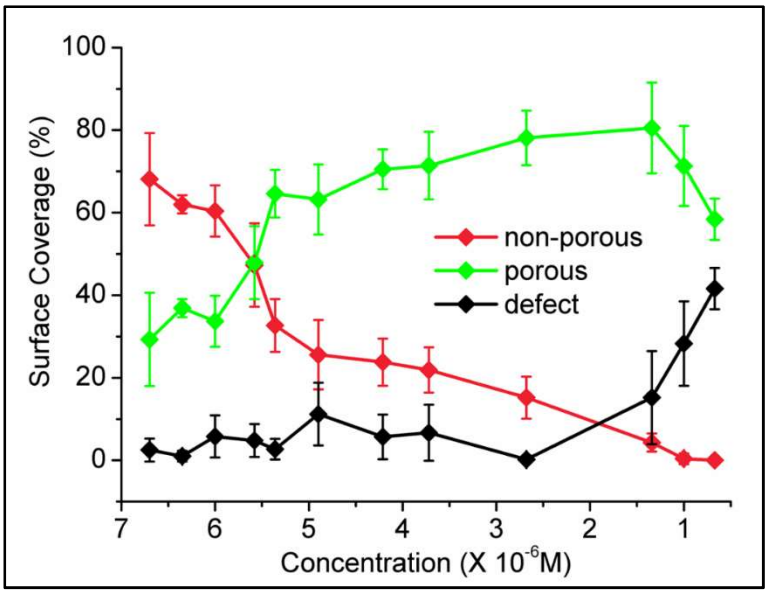

Figure S4. Concentration dependent surface coverage of porous (green) and non-porous (red) phase of DBA-OC13 at the 1-phenyloctane/pristine HOPG interface. At lower concentrations, defects in the monolayer (black) start to appear.

For each DBA-OC13 concentration studied, detailed information regarding the total scanning area analysed and the average surface coverage (%) for porous, non-porous and defects on the monolayer are available in the table below.

Table S1. Surface coverage for DBA-OC13 at the 1-phenyloctane/graphite interface, at different concentrations.

Concentration (M)	Total scanning area (nm^2)	Total number of images	Area (nm^2)			Average surface coverage ± standard deviation (s. d.) (%)					
			Non-porous	Porous	Defect	**Non-porous**	s. d.	**Porous**	s. d.	Defect	s. d.
6.7×10^{-4}	130000	13	118794	11206	0	**91.6**	1.0	**8.4**	1.0	0	0
6.7×10^{-5}	80000	8	70343	8647	1010	**87.5**	1.5	**11.2**	1.5	1.3	0.2
6.7×10^{-6}	70000	7	47699	20544	1757	**68.1**	11.2	**29.3**	11.3	2.5	2.8
6.35×10^{-6}	170000	17	105479	62799	1722	**62.0**	2.2	**36.9**	2.2	1.0	1.3
6.0×10^{-6}	200000	20	120882	67489	11629	**60.4**	6.2	**33.7**	6.2	5.8	5.1
5.6×10^{-6}	290000	29	137207	139010	13783	**47.3**	10.1	**47.9**	8.8	4.8	4.0
5.36×10^{-4}	300000	30	98114	193933	7953	**32.7**	6.4	**64.6**	5.8	2.7	2.5
4.9×10^{-5}	140000	14	35859	88488	15653	**25.6**	8.4	**63.2**	8.5	11.2	7.6
4.21×10^{-6}	120000	12	28588	84590	6822	**23.8**	5.7	**70.5**	4.8	5.7	5.4
3.72×10^{-6}	210000	21	45956	150020	14024	**21.9**	5.5	**71.4**	8.2	6.7	6.8
2.68×10^{-6}	200000	20	30467	156206	13327	**15.2**	5.1	**78.1**	6.6	0.2	0.1
1.34×10^{-6}	140000	14	5951	112754	21295	**4.3**	2.2	**80.5**	11.0	15.2	11.3
1.0×10^{-6}	360000	9	1520	256600	101880	**0.4**	1.3	**71.3**	9.7	28.3	10.2
6.7×10^{-7}	340000	13	0	194987	145013	**0**	0	**58.4**	5.0	41.6	5.0

In the table below (Table S2), there is an example which shows the determination of the surface coverage for each STM image obtained with a DBA-OC13 concentration of 5.6×10^{-6} M.

Table S2. Statistics for the surface coverage of porous and non-porous phase for DBA-OC13 (5.6×10^{-6} M) at the 1-phenyloctane/graphite interface.

Image	Scanning area (nm^2)	No. of pores	Area for a single pore (nm^2)	Area (nm^2)			Surface coverage (%)		
				Non-porous	Porous	Defect	Non-porous	Porous	Defect
1	10000	200	22	5210	4400	390	52.1	44.0	3.9
2	10000	220	23	4024	5060	916	40.2	50.6	9.2
3	10000	237	24	3694	5688	618	36.9	56.9	6.2
4	10000	196	24	4650	4704	646	46.5	47.0	6.5
5	10000	128	22	7184	2816	0	71.8	28.2	0
6	10000	150	25	6056	3750	194	60.6	37.5	1.9
7	10000	194	22	4314	4268	1418	43.1	42.7	14.2
8	10000	195	23	4911	4485	604	49.1	44.9	6.0
9	10000	213	22	5080	4686	234	50.8	46.9	2.3
10	10000	141	26	5402	3666	932	54.0	36.7	9.3
11	10000	184	22	5504	4048	448	55.0	40.5	4.5
12	10000	166	24	5505	3984	511	55.1	39.8	5.1
13	10000	213	21	5527	4473	0	55.3	44.7	0
14	10000	206	22	4801	4532	667	48.0	45.3	6.7
15	10000	145	25	6242	3625	133	62.4	36.3	1.3
16	10000	232	22	4763	5104	133	47.6	51.0	1.3
17	10000	225	25	4080	5625	293	40.8	56.3	2.9
18	10000	235	22	4686	5170	144	46.9	51.7	1.4
19	10000	249	25	3317	6225	458	33.2	62.3	4.6
20	10000	203	24	4889	4872	239	48.9	48.7	2.4
21	10000	234	26	3530	6084	386	35.3	60.8	3.9
22	10000	240	23	3415	5520	1065	34.2	55.2	10.7
23	10000	237	22	3567	5214	1219	35.7	52.1	12.2
24	10000	161	22	6458	3542	0	64.6	35.4	0
25	10000	217	23	4870	4991	139	48.7	49.9	1.4
26	10000	239	22	3501	5258	1241	35.0	52.6	12.4
27	10000	277	24	3109	6648	243	31.1	66.5	2.4
28	10000	215	24	4447	5160	393	44.5	51.6	3.9
29	10000	246	22	4469	5412	119	44.7	54.1	1.2
Total	**290000**	**5998**	–	**137207**	**139010**	**13783**	–	–	–
Average	–	**207**	–	–	–	–	**47.3**	**47.9**	**4.8**
s. d.	–	**37**	–	–	–	–	**10.1**	**8.8**	**4.0**

S5. Experimental details on corral fabrication

S5.1 Covalent modification of HOPG

Electrochemical grafting of 3,4,5-trimethoxybenzenediazonium (3,4,5-TMD, concentration: ≥ 2mM) was performed using cyclic voltammetry in aqueous solutions, using an Autolab PGSTAT101 (Metrohm Autolab BV, The Netherlands). Before each experiment, the HOPG was freshly cleaved using scotch tape. The electrochemical modification procedure was carried out in a homemade single-compartment three-electrode cell with a working electrode area of 50.3 mm^2, Pt wire counter and Ag/AgCl/3 M NaCl reference electrodes. 3,4,5-trimethoxybenzenediazonium (3,4,5-TMeOD) chloride is unstable and decomposes rapidly: hence it was synthesized from the corresponding aniline precursor immediately prior to electrochemical reduction. This procedure involves 5 mL of a 2 mM 3,4,5-trimethoxyaniline (97%, Sigma-Aldrich) in 50 mM HCl (Sigma-Aldrich) aqueous solution which was mixed with 100 μL of aqueous $NaNO_2$ (0.1 M) for activation of the diazotization reaction. Within 3 minutes this mixture was gently shaken and pipetted into the EC cell. Cyclic voltammetry (3 cycles, range: 0.5V to −0.6V, scanning rate: 100 mV/s) was used for the electrochemical activation. After modification, TBP modified samples were rinsed with Milli-Q water (Milli-Q, Millipore, 18.2 MΩ cm, TOC < 3 ppb) to remove any physisorbed material from the surface and dried in a stream of Argon. All chemical compounds were used without further purification.

S5.2 Corral fabrication

Before nanoshaving, densely and randomly packed 3,4,5-TMDs were grafted on the HOPG surface following the protocol described before. All corrals were created with a detailed control over the nanoshaving process using the Keysight PicoLITH 2.1 software package.[3-5] First, different shapes (square, circles and triangles) for the creation of nanocorrals were designed within this software. During the nanoshaving process, the STM was operating under high current (200 pA) and low sample bias (−1.0 mV) conditions. These scanning parameters bring the tip in close proximity to the graphite substrate, such that the covalently bound aryls are removed from the HOPG surface. The tip speed for nanoshaving was set to 400 nm/s.

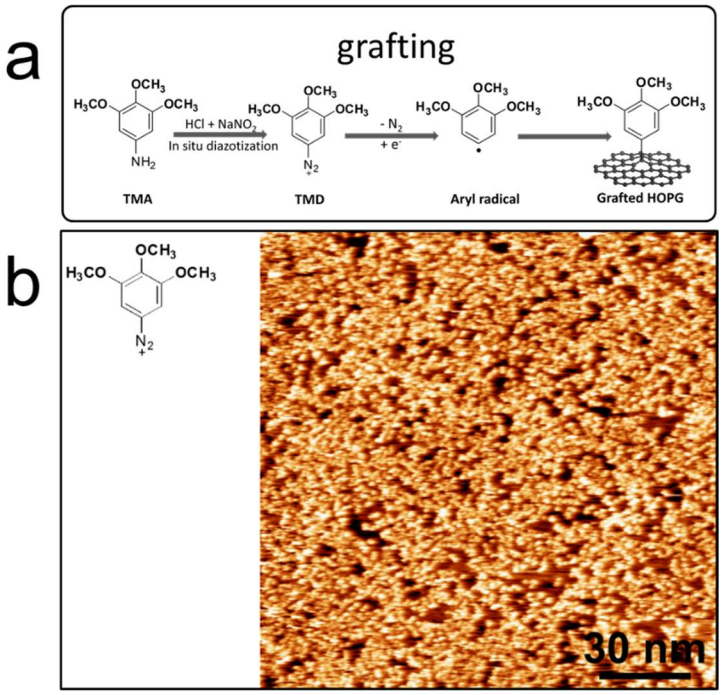

Figure S5. (a) Reaction scheme for the grafting of 3,4,5-TMeOD onto HOPG. (b) Large-scale STM image for the HOPG surface covalently modified by 3,4,5-trimethoxyphenyls. Scanning parameters: V_s = –0.80 V, I_t = 80 pA.

S6. Surface coverage of DBA-OC13 in corrals of different sizes

The DBA-OC13 molecules adsorb in the corrals and form self-assembled monolayers, the area of which is defined by the size of the nanocorrals (Fig. 3a, b of the main text). For the larger nanocorrals, it is impossible to identify the self-assembly structures without zooming in (at 50 × 50 nm2). Repeating this nanoshaving process many times on different locations for each of the nanocorral sizes, rendered average values for the surface coverage of the porous phase.

S6.1 Data for smaller corrals

Table S3. Detailed statistics of the porous surface coverage of DBA-OC13 (5.6×10^{-6} M) in smaller corrals, where confinement effects are more pronounced.

Image	Square corrals (24 nm)				Square corrals (39 nm)				Square corrals (60 nm)			
	Corral area (nm^2)	No. of pores	Total area for porous structure (nm^2)	**Surface coverage for porous structure (%)**	Corral area (nm^2)	No. of pore	Area for porous structure (nm^2)	**Surface coverage for porous structure (%)**	Corral area (nm^2)	No. of pore	Area for porous structure (nm^2)	**Surface coverage for porous structure (%)**
1	474	3	54	**11.4**	1295	8	144	**11.1**	3289	21	441	**13.4**
2	476	2	36	**7.6**	1289	7	126	**9.8**	3039	14	294	**9.7**
3	486	3	54	**11.1**	1376	8	144	**10.5**	3230	26	546	**16.9**
4	539	3	54	**10.0**	1632	11	198	**12.1**	3347	17	357	**10.7**
5	727	2	36	**5.0**	1756	7	126	**7.2**	3807	23	483	**12.7**
6	758	2	36	**4.7**	1752	8	144	**8.2**	4255	15	315	**7.4**
7	614	2	36	**5.9**	1637	4	72	**4.4**	3676	26	546	**14.9**
8	588	2	36	**6.1**	1591	4	72	**4.5**	3605	16	336	**9.3**
9	719	2	36	**5.0**	1655	10	180	**10.9**	4489	22	462	**10.3**
10	560	3	54	**9.6**	1516	12	216	**14.2**	4541	17	357	**7.9**
11	585	1	18	**3.1**	1087	7	126	**11.6**	2607	19	399	**15.3**
12	625	1	18	**2.9**	1711	13	234	**13.7**	3906	17	357	**9.0**
13	587	4	72	**12.3**	1516	8	144	**9.5**	3491	13	273	**7.8**
14	588	2	36	**6.1**	1375	10	180	**13.1**	3409	5	105	**3.1**
15	662	2	36	**5.4**	1600	7	126	**7.9**	3530	20	420	**11.9**

S6.2 Data for larger corrals

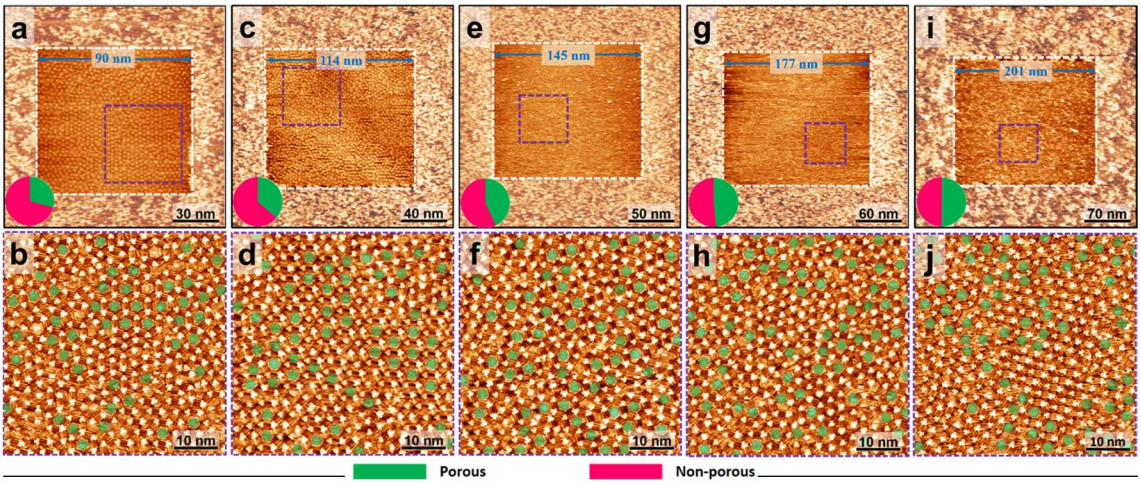

Figure S6. Large-scale (top row) and zoomed-in STM (bottom row) images showing the self-assemblies of DBA-OC13 (5.6×10^{-6} M) in square corrals of different size. (a, c, e, g and i) The size is indicated in the corrals. Scanning parameters: V_s = –0.80 V, I_t = 80 pA. (b, d, f, h and j) Zoomed-in images of the self-assembly of DBA-OC13 in the nanocorrals above. Scan size is 50 × 50 nm^2. Porous structures are indicated by green dots. Scanning parameters: V_s = –0.20 V, I_t = 300 pA. The pie charts reveal the relative surface coverage of the porous (green) and non-porous (red) phases, based on the average of 40 images, obtained from 10 nanocorrals.

Table S4. Average surface coverage (%) for the porous/non-porous phase of DBA-OC13 (5.6×10^{-6} M) in square corrals of different sizes.

Corral size (nm)		Average No. of pores in corrals	Average No. of pores in zoomed areas (50 × 50 nm^2)	Average area for porous structure (nm^2)	Average surface coverage ± s. d. (%)			
Average side length ± s. d.					**Non-porous**	s. d.	**Porous**	s. d.
24	2	2.3	–	43	**92.9**	3.1	**7.1**	3.1
39	3	8.3	–	150	**90.1**	3.0	**9.9**	3.0
60	4	18.1	–	387	**89.3**	3.6	**10.7**	3.6
90	6	–	36.7	697	**72.1**	7.4	**27.9**	7.4
114	4	–	52.0	972	**61.1**	8.0	**38.9**	8.0
145	3	–	59.8	1156	**53.7**	4.6	**46.3**	4.6
177	6	–	62.4	1226	**50.9**	4.3	**49.1**	4.3
201	4	–	63.3	1252	**49.9**	5.2	**50.1**	5.2

For every corral size, we use in total forty 50 × 50 nm^2 images for calculating the surface coverage of the porous/non-porous phase. Table S5 shows detailed information on the statistics obtained for 114×114 nm^2 corral, as an example.

Table S5. Detailed statistics for the porous/non-porous surface coverage of DBA-OC13 (5.6×10^{-6} M) in corrals of 114×114 nm^2.

Image	Corral	Zoom area (nm^2)	No. of pores	Area for 1 pore	Area (nm^2)		**Surface coverage (%)**	
					Non-porous	Porous	**Non-porous**	**Porous**
1	1	2500	57	19	1417	1083	**56.7**	**43.3**
2		2500	40	19	1740	760	**69.6**	**30.4**
3		2500	39	19	1759	741	**70.4**	**29.6**
4	2	2500	40	20	1700	800	**68.0**	**32.0**
5		2500	41	20	1680	820	**67.2**	**32.8**
6		2500	41	19	1721	779	**68.8**	**31.2**
7		2500	34	19	1854	646	**74.2**	**25.8**
8	3	2500	54	17	1582	918	**63.3**	**36.7**
9		2500	46	17	1718	782	**68.7**	**31.3**
10		2500	58	18	1456	1044	**58.2**	**41.8**
11	4	2500	52	18	1564	936	**62.6**	**37.4**
12		2500	57	19	1417	1083	**56.7**	**43.3**
13	5	2500	52	17	1616	884	**64.6**	**35.4**
14		2500	55	17	1565	935	**62.6**	**37.4**
15		2500	36	17	1888	612	**75.5**	**24.5**
16		2500	42	18	1744	756	**69.8**	**30.2**
17	6	2500	62	20	1260	1240	**50.4**	**49.6**
18		2500	60	19	1360	1140	**54.4**	**45.6**
19		2500	56	20	1380	1120	**55.2**	**44.8**
20		2500	38	20	1740	760	**69.6**	**30.4**
21	7	2500	69	20	1120	1380	**44.8**	**55.2**
22		2500	75	20	1000	1500	**40.0**	**60.0**
23		2500	67	19	1227	1273	**49.1**	**50.9**
24		2500	58	19	1398	1102	**55.9**	**44.1**
25	8	2500	36	18	1852	648	**74.1**	**25.9**
26	9	2500	53	18	1546	954	**61.8**	**38.2**
27		2500	53	18	1546	954	**61.8**	**38.2**
28		2500	60	18	1420	1080	**56.8**	**43.2**
29		2500	45	17	1735	765	**69.4**	**30.6**
30	10	2500	57	18	1474	1026	**59.0**	**41.0**

31		2500	56	17	1548	952	**61.9**	**38.1**
32		2500	54	17	1582	918	**63.3**	**36.7**
33		2500	57	19	1417	1083	**56.7**	**43.3**
34	11	2500	57	19	1417	1083	**56.7**	**43.3**
35		2500	53	19	1493	1007	**59.7**	**40.3**
36		2500	49	20	1520	980	**60.8**	**39.2**
37		2500	50	20	1500	1000	**60.0**	**40.0**
38	12	2500	52	20	1460	1040	**58.4**	**41.6**
39		2500	62	20	1260	1240	**50.4**	**49.6**
40		2500	55	19	1455	1045	**58.2**	**41.8**

S6.3 Data for different concentrations

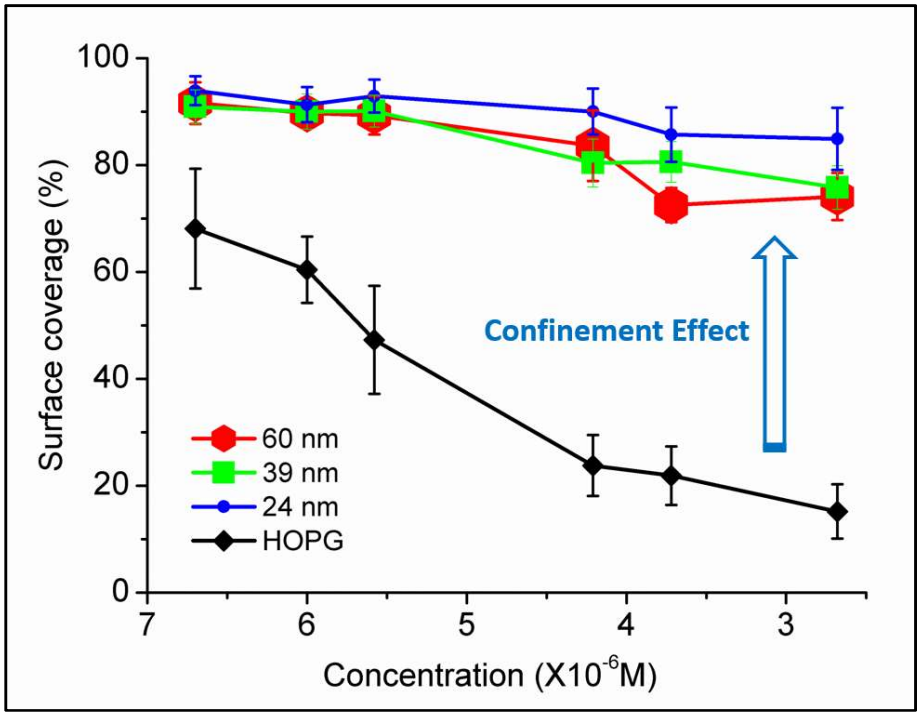

Figure S7. Dependence of surface coverage of the non-porous structure of DBA-OC13 on concentration in 1-phenyloctane, as experimentally addressed for bare HOPG (black), and in square corrals with average size of 24 (blue), 39 (green), and 60 nm (red). Each data point is the average of 15 images from different positions.

S7. Concentration dependence phase behaviour for DBA-OC12 on pristine HOPG

For every concentration studied, 15 to 30 images obtained during 2-3 experimental sessions were used for the porous/non-porous surface coverage determination. Each point represents an average value, while the error bars represent the standard deviation.

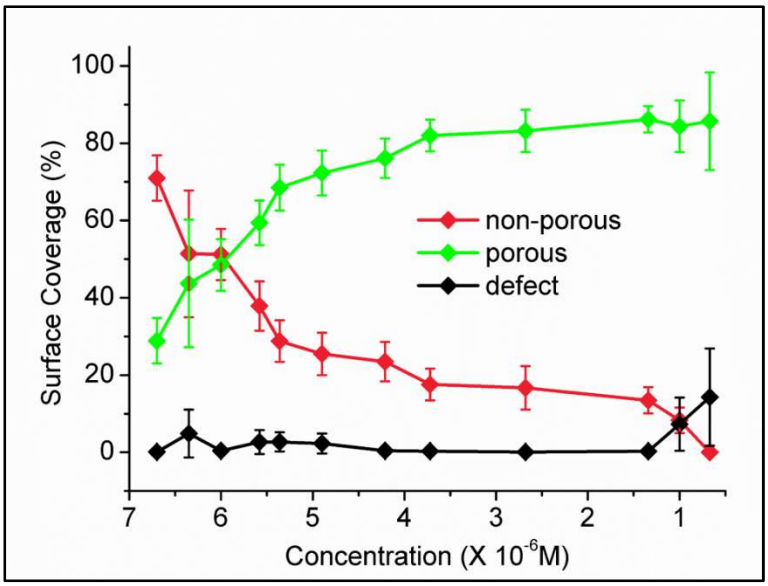

Figure S8. Concentration dependent surface coverage of porous (green) and non-porous (red) phase of DBA-OC12 at the 1-phenyloctane/pristine HOPG interface.

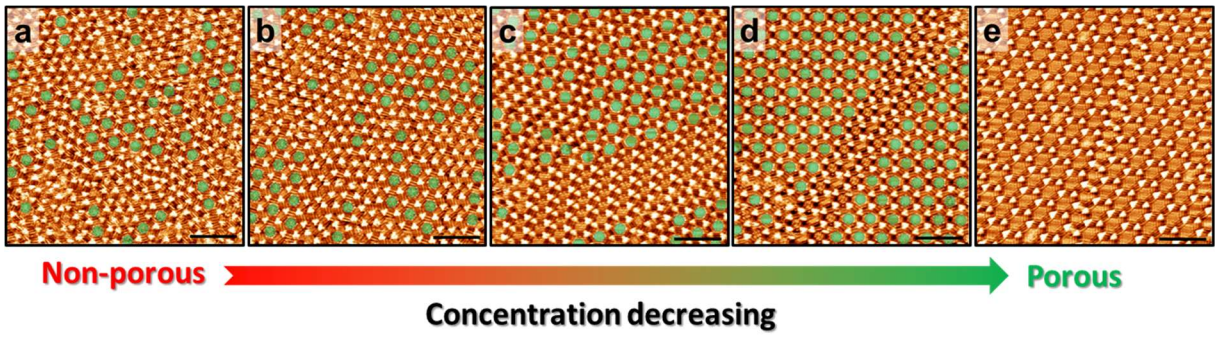

Figure S9. Representative large-scale STM images for DBA-OC12 showing the phase transition from non-porous to porous phase. Concentration: (a) 6.7×10^{-4} M; (b) 6.7×10^{-6} M; (c) 6.0×10^{-6} M; (d) 2.68×10^{-6} M; (e) 6.7×10^{-7} M. Scanning parameters: $V_s = -0.20$ V, $I_t = 300$ pA. Scale bar is 10 nm.

S8. Surface coverage of DBA-OC12 in corrals of different sizes

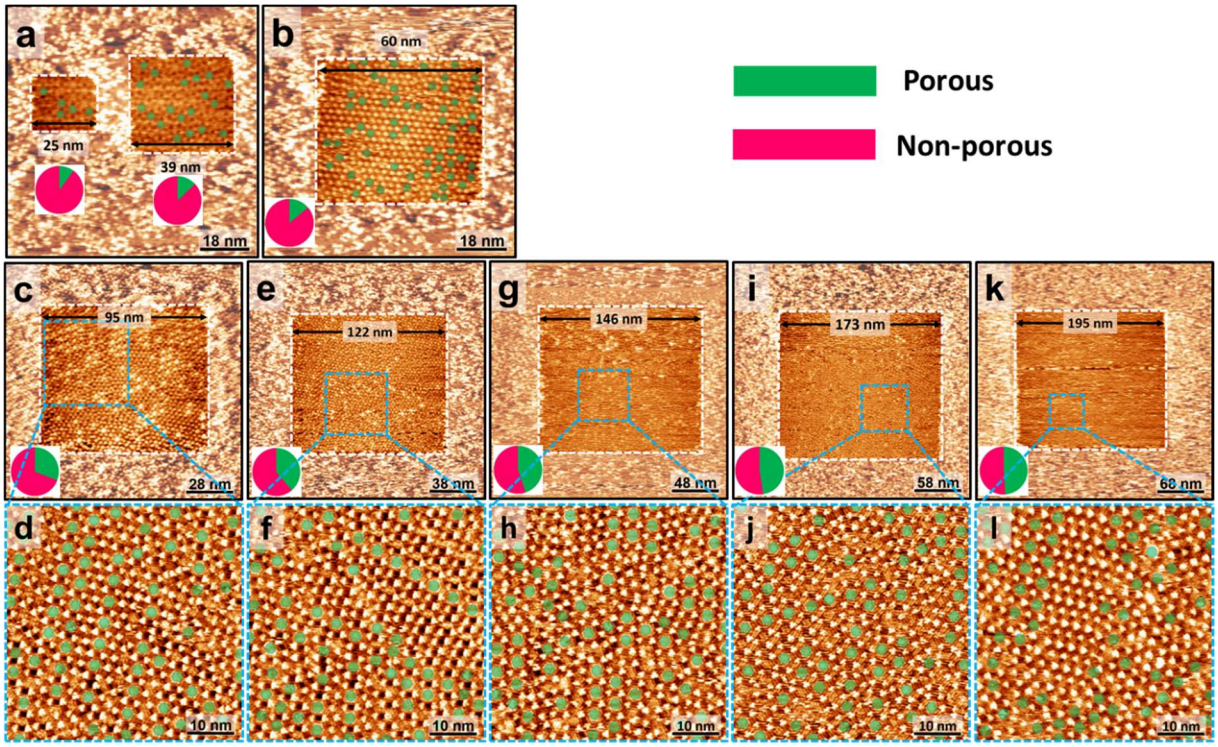

Figure S10. Large-scale and zoomed STM images showing the self-assemblies of DBA-OC12 (6.0×10^{-6} M) in corrals with different sizes. Porous structures are indicated by green dots. The pie charts reveal the relative surface coverage of the porous (green) and non-porous (red) phases. Scanning parameters: (a, b, c, e, g, I and k) $V_s = -0.80$ V, $I_t = 80$ pA; (d, f, h, j and l) $V_s = -0.20$ V, $I_t = 300$ pA.

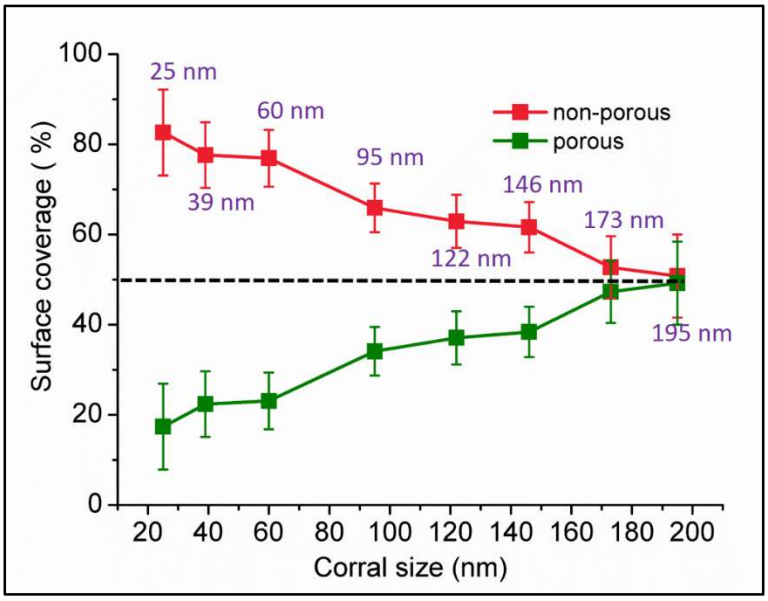

Figure S11. Dependence of the surface coverage of porous and non-porous structures of DBA-OC12 (6.0×10^{-6} M) as a function of the size of the square corrals. For every corral size, forty 50 × 50 nm^2 images were used for porous/non-porous surface coverage determination.

Table S6. Average surface coverage (%) for the porous/non-porous phase of DBA-OC12 (6.0×10^{-6} M) in square corrals of different sizes

Corral size (nm)		Average No. of pores in corrals	Average No. of pores in zoomed areas (50 × 50 nm^2)	Average area for porous structure (nm^2)	Average surface coverage ± s. d. (%)			
Average side length ± s. d.					**Non-porous**	s. d.	**Porous**	s. d.
25	1	5.6	–	104	**82.6**	9.5	**17.4**	9.5
39	1	18.9	–	342	**77.6**	7.3	**22.4**	7.3
60	2	45.1	–	818	**76.9**	6.3	**23.1**	6.3
95	4	–	46.1	852	**65.9**	5.4	**34.1**	5.4
122	4	–	50.3	929	**62.9**	5.9	**37.1**	5.9
146	5	–	51.4	960	**61.6**	5.6	**38.4**	5.6
173	5	–	61.5	1183	**52.7**	6.9	**47.3**	6.9
195	5	–	63.1	1229	**50.8**	9.2	**49.2**	9.2

S9. Self-assembly of DBA-OC13 in circular and triangular corrals

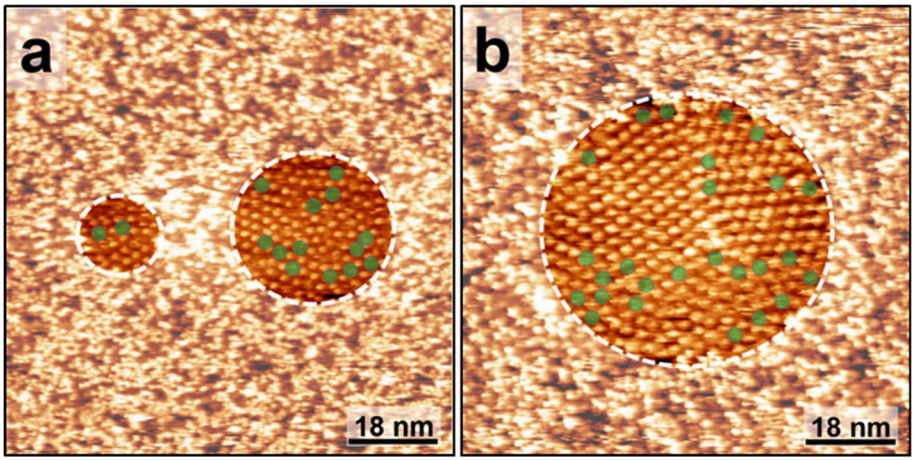

Figure S12. (a, b) STM images for the self-assembly of DBA-OC13 (5.6×10^{-6} M) in circular nanocorrals of different size. The diameter of these nanocorrals is 22 ± 2 nm and 40 ± 1 nm in (a), and 61 ± 5 nm in (b). Porous structures are indicated by green dots. Scanning parameters: V_s = – 0.80 V, I_t = 80 pA.

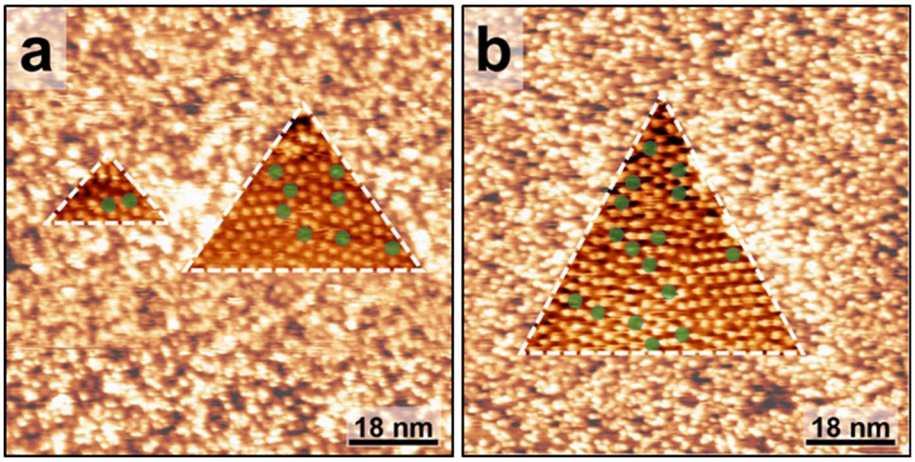

Figure S13. (a, b) STM images for the self-assembly of DBA-OC13 (5.6×10^{-6} M) in triangular corrals of different size. The side of these nanocorrals measures 31 ± 6 nm and 48 ± 7 nm in (a) and 69 ± 4 nm in (b). Porous structures are indicated by green dots. Scanning parameters: V_s = – 0.80 V, I_t = 80 pA.

Conclusion: irrespective of the nanocorral shape, the non-porous phase is favored in the corrals.

S10. Stability of nanoconfined DBA-OC13 assemblies over time

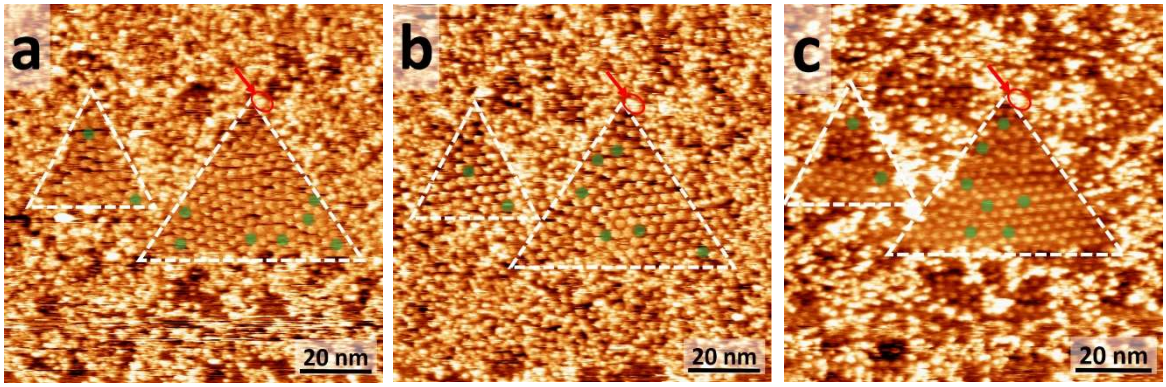

Figure S14. STM-images of DBA-OC13 (2.68×10^{-6} M) at the 1-phenyloctane/HOPG interface. The time-interval between image a and b is 15 minutes, and between b and c is 11 minutes. The images were obtained under continuous scanning. The green dots indicate the porous phase. The red arrow points at a distinguishable surface feature for reference. Scanning parameters: V_s = -0.80 V, I_t = 80 pA.

Conclusion: While dynamics were occasionally observed, the porous : non-porous ratio remained unaltered.

S11. Data for *in situ* nanoshaving at elevated temperature

In situ nanoshaving in the presence of DBA-OC13 (5.6×10^{-6} M in 1-phenyloctane) was performed at both room temperature and at 50 °C. In order to contain the solution over longer periods of time, a liquid cell was mounted on top of the sample. 2 to 3 droplets of solution were added to the liquid cell at room temperature prior to nanoshaving/imaging. First, nanocorrals were created at room temperature. Next, the sample was heated to 50 °C using a LakeShore 331 Temperature Controller and left at this temperature for ~10 minutes in order to stabilize. Nanocorrals were subsequently made and imaged at 50 °C. The results are given in Table S7.

Table S7. Surface composition of self-assembled phases formed by DBA-OC13 (5.6×10^{-6} M in 1-phenyloctane) inside *in situ* created square nanocorrals at room temperature and at 50 °C. 8 corrals (23.9 nm) and 8 corrals (36.1 nm) were investigated at room temperature; 13 corrals (23.9 nm) and 14 corrals (36.1 nm) were investigated at 50°C. At least two samples were investigated for each reported value. Errors represent the standard deviation.

Corral width (nm)	Phase	Surface composition (%)	
		T_{room}	50 °C
23.9 ± 2.9	Porous	23.3 ± 4.0	15.3 ± 13.6
	Linear	76.7 ± 4.0	84.7 ± 13.6
	Defect	0	0
36.1 ± 3.0	Porous	18.7 ± 6.3	14.9 ± 11.9
	Linear	81.3 ± 6.3	84.6 ± 12.4
	Defect	0	0.5 ± 1.7

Conclusion: The nanoconfined surface composition of DBA-OC13 at 50 °C is not significantly different from that at room temperature.

S12. Control experiment – Dependence on the nanoshaving direction

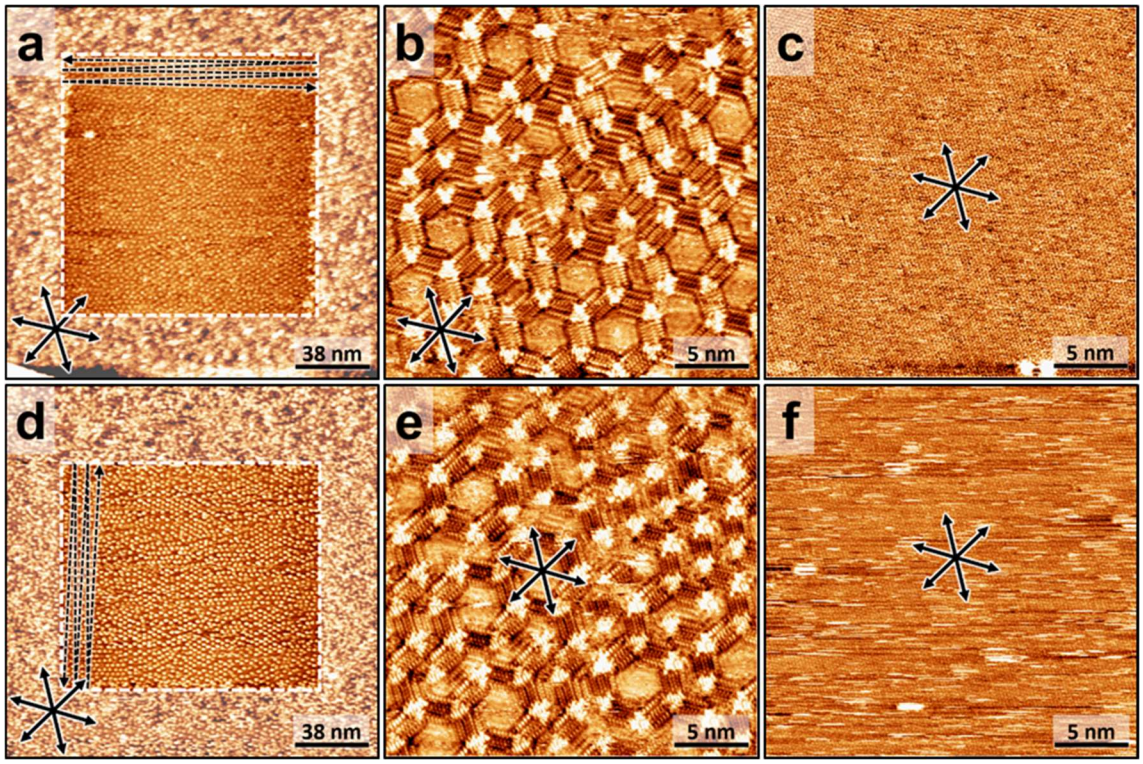

Figure S15. Self-assembly of DBA-OC13 (5.6×10^{-6} M) in square corrals, under different nanoshaving directions (represented by the dotted arrows in (a) and (d)). The main symmetry axis of HOPG are defined by the black arrows. Panels (b) and (e) show zoomed-in images obtained inside corrals (a) and (b). Panel (c) and (f) show the HOPG lattice obtained in the same location as the previous images. Scanning parameters: V_s = –0.80 V, I_t = 80 pA for panel (a) and (d); V_s = –0.20 V, I_t = 300 pA for panel (b) and (e); V_s = –0.20 V, I_t = 1 pA for panel (c) and (f).

Conclusion: The packing of DBA molecules is determined by the orientation of the HOPG lattice, namely, the alkyl chains are extended along one of the symmetry axes of the HOPG lattice.

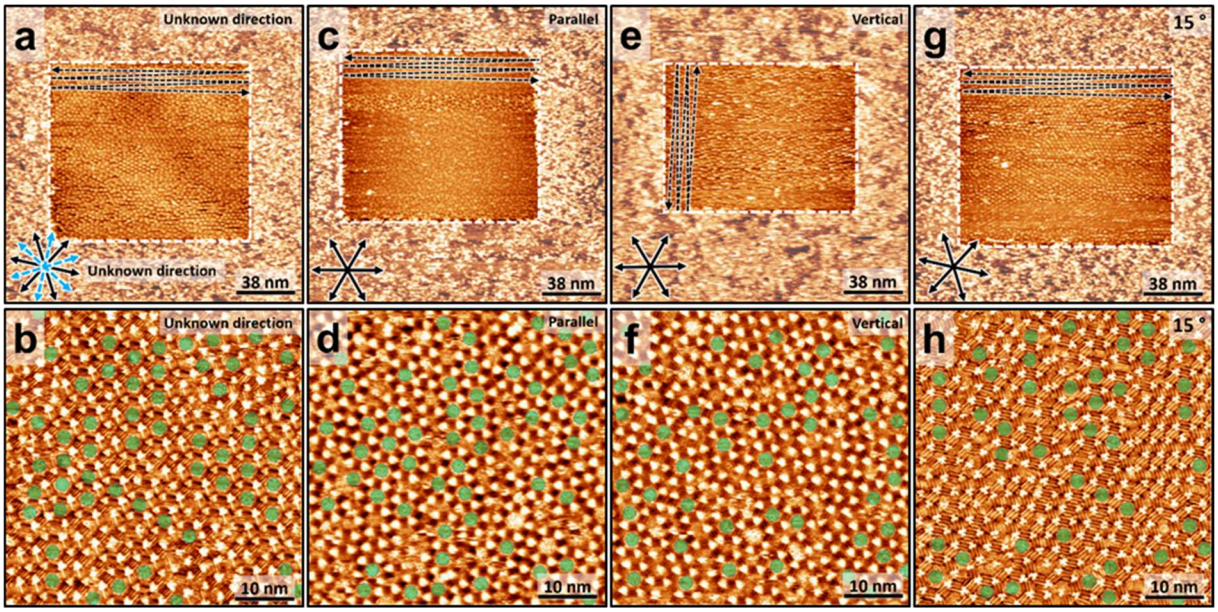

Figure S16. Large-scale and zoomed-in STM images showing the self-assembly of DBA-OC13 (5.6×10^{-6} M) in corrals where the direction of the nanoshaving process was controlled with respect to one of the main symmetry axes of HOPG. (a, b) unknown direction; (c, d) parallel direction (0°); (e, f) vertical direction (90°); (g and h) 15° to one of the main symmetry axis of HOPG. Scanning parameters: (a, c, e, g) $V_s = -0.80$ V, $I_t = 80$ pA; (b, d, f, h) $V_s = -0.20$ V, $I_t = 300$ pA.

Table S8. Summary of the surface coverage for porous and non-porous structures in corrals created under different nanoshaving directions with respect to the HOPG lattice.

Nanoshaving direction	Non-porous	Porous	Number of images
Unknown	61.1 ± 8.0 %	38.9 ± 8.0 %	40
Parallel (0°)	60.2 ± 4.5 %	39.8 ± 4.5 %	18
Vertical (90°)	59.6 ± 5.2 %	40.4 ± 5.2 %	17
15°	60.4 ± 4.3 %	39.6 ± 4.3 %	30

Conclusion: The relative surface coverage for the porous and non-porous phases is not influenced by the nanoshaving direction.

S13. References

1. K. Tahara, S. Furukawa, H. Uji-i, T. Uchino, T. Ichikawa, J. Zhang, W. Mamdouh, M. Sonoda, F. C. De Schryver, S. De Feyter and Y. Tobe, *Journal of the American Chemical Society*, 2006, **128**, 16613-16625.
2. K. Tahara, C. A. Johnson, T. Fujita, M. Sonoda, F. C. De Schryver, S. De Feyter, M. M. Haley and Y. Tobe, *Langmuir : the ACS journal of surfaces and colloids*, 2007, **23**, 10190-10197.
3. L. Verstraete, J. Greenwood, B. E. Hirsch and S. De Feyter, *ACS Nano*, 2016, **10**, 10706-10715.
4. L. Verstraete, B. E. Hirsch, J. Greenwood and S. De Feyter, *Chemical communications*, 2017, **53**, 4207-4210.
5. J. Greenwood, T. H. Phan, Y. Fujita, Z. Li, O. Ivasenko, W. Vanderlinden, H. Van Gorp, W. Frederickx, G. Lu, K. Tahara, Y. Tobe, H. Uji-i, S. F. L. Mertens and S. De Feyter, *ACS Nano*, 2015, **9**, 5520-5535.